



## NRC Publications Archive Archives des publications du CNRC

### **14N magic angle spinning overtone NMR spectra** O'Dell, Luke A.; Ratcliffe, Christopher I.

This publication could be one of several versions: author's original, accepted manuscript or the publisher's version. / La version de cette publication peut être l'une des suivantes : la version prépublication de l'auteur, la version acceptée du manuscrit ou la version de l'éditeur.

For the publisher's version, please access the DOI link below. / Pour consulter la version de l'éditeur, utilisez le lien DOI ci-dessous.

#### **Publisher's version / Version de l'éditeur:**

<https://doi.org/10.1016/j.cplett.2011.08.030>

*Chemical Physics Letters*, 514, 1-3, pp. 168-173, 2011-08-17

#### **NRC Publications Record / Notice d'Archives des publications de CNRC:**

<https://nrc-publications.canada.ca/eng/view/object/?id=c12dd79b-a105-43f7-86a2-8444f0a0d867>

<https://publications-cnrc.canada.ca/fra/voir/objet/?id=c12dd79b-a105-43f7-86a2-8444f0a0d867>

Access and use of this website and the material on it are subject to the Terms and Conditions set forth at

<https://nrc-publications.canada.ca/eng/copyright>

READ THESE TERMS AND CONDITIONS CAREFULLY BEFORE USING THIS WEBSITE.

L'accès à ce site Web et l'utilisation de son contenu sont assujettis aux conditions présentées dans le site

<https://publications-cnrc.canada.ca/fra/droits>

LISEZ CES CONDITIONS ATTENTIVEMENT AVANT D'UTILISER CE SITE WEB.

#### **Questions?** Contact the NRC Publications Archive team at

PublicationsArchive-ArchivesPublications@nrc-cnrc.gc.ca. If you wish to email the authors directly, please see the first page of the publication for their contact information.

**Vous avez des questions?** Nous pouvons vous aider. Pour communiquer directement avec un auteur, consultez la première page de la revue dans laquelle son article a été publié afin de trouver ses coordonnées. Si vous n'arrivez pas à les repérer, communiquez avec nous à PublicationsArchive-ArchivesPublications@nrc-cnrc.gc.ca.



# **$^{14}\text{N}$ Magic Angle Spinning Overtone NMR Spectra**

Luke A. O'Dell\* and Christopher I. Ratcliffe

Steacie Institute for Molecular Sciences, National Research Council Canada,  
100 Sussex Drive, Ottawa, ON, Canada, K1A 0R6

Email: [luke.odell@nrc-cnrc.gc.ca](mailto:luke.odell@nrc-cnrc.gc.ca)

Tel: 1-613-990-1566

## **Abstract**

We present the first  $^{14}\text{N}$  overtone NMR spectra obtained directly under magic angle spinning conditions. Line-broadening contributions from chemical shift anisotropy and heteronuclear dipolar couplings are significantly reduced, and, despite theoretical predictions, spinning sidebands are minimal, leaving second-order quadrupolar powder patterns with narrow discontinuities that can be observed using a single excitation pulse. We also show that the limited bandwidth and offset-dependent nutation rates exhibited by standard RF pulses can be overcome using frequency-swept pulses, allowing the direct acquisition of solid-state  $^{14}\text{N}$  NMR spectra in which multiple nitrogen sites are well resolved.

## 1. Introduction

Nitrogen is one of the most important and abundant elements in nature, yet solid-state nuclear magnetic resonance (NMR) studies of the 99.6 % naturally abundant  $^{14}\text{N}$  nucleus are scarce. This is due to the combination of its moderate quadrupole moment (20.4 mbarn) and integer spin number ( $I = 1$ ), which results in very large first-order quadrupolar perturbations to the  $\Delta m = 1$  (fundamental) Zeeman transitions, broadening the resonances over many MHz for the vast majority of nitrogen sites and making standard magic angle spinning (MAS) experiments very difficult [1,2]. A variety of experimental approaches have been proposed to allow the extraction of useful information from this difficult nucleus (see recent reviews [1,3] and references therein), but so far none of these methods have become routine.

Several decades ago, Bloom & LeGros noted that the first-order quadrupolar perturbation is absent from the  $\Delta m = 2$ , or “overtone” transition and that this transition is weakly allowed when the magnitudes of the quadrupolar and Zeeman interactions are comparable [4]. Shortly after, Tycko & Opella reported the first  $^{14}\text{N}$  overtone NMR spectra from single-crystal and powder samples [5,6]. The absence of the first-order quadrupolar interaction vastly reduces the spectral range, and for single-crystal samples results in very narrow linewidths that can be easily acquired. For polycrystalline samples, however, the second-order quadrupolar interaction (SOQI) and chemical shift anisotropy (CSA) can broaden the overtone powder patterns across ranges of several tens of kHz or more. This reduces the resolution and sensitivity, and when using single-pulse experiments the receiver dead-time (between the excitation pulse and the start of the acquisition) can make these wide patterns very difficult to obtain without severe distortions and signal loss. Ordinarily, the dead-time problem can be overcome using spin-echo methods, but the very slow nutation rates exhibited by overtone magnetization, combined with the dependence of the nutation frequency on the magnitude and orientation of the quadrupolar interaction, makes overtone spin-echo experiments very challenging. Moreover, the excitation of the overtone transition becomes less efficient at higher magnetic field strengths.

In this letter, we show that MAS can be used to reduce the effects of the CSA and heteronuclear dipolar couplings, thereby narrowing the overtone powder patterns at

moderate or high magnetic fields and allowing straightforward single-pulse experiments in which signal loss due to the dead-time is mitigated. Surprisingly, no experimental MAS overtone spectra have been reported before.  $^{14}\text{N}$  overtone spectra have been obtained from a sample of N-acetylvaline spinning at other angles with respect to the magnetic field [6], but these exhibited poor signal-to-noise ratios and showed broader linewidths than the static spectra. Takegoshi & Hikichi alluded to the advantages of MAS almost 20 years ago [7], but subsequent theoretical analyses concluded that sample spinning in overtone NMR would result in broad and intense spinning sideband-like features and/or significant signal loss due to cancellations induced by the sample rotation [8,9]. Here we show that, on the contrary, MAS overtone  $^{14}\text{N}$  spectra can be obtained with minimal (or no) sidebands and can exhibit the same level of signal intensity as static spectra. Additionally, we demonstrate that a frequency-swept pulse can provide an improved excitation bandwidth and can overcome nutation problems related to transmitter offsets, thereby allowing the acquisition of spectra in which signals from multiple sites are well-resolved.

## 2. Experimental details

All  $^{14}\text{N}$  overtone spectra were obtained at 11.7 T using a 500 MHz Bruker Avance III spectrometer and a Varian double-resonance T3 probe with a 4.0 mm o.d. rotor size. Spectra were recorded using single-pulse excitation at an RF power corresponding to a nutation rate of  $\nu_1 = 42$  kHz for the fundamental  $^{14}\text{N}$  transitions. This power was indirectly determined using  $^2\text{H}$  nuclei, which are close in frequency to the  $^{14}\text{N}$  overtone transition. Spectra are referenced against the fundamental  $^{14}\text{N}$  signal from solid  $\text{NH}_4\text{Cl}$  such that 0 kHz corresponds to exactly twice this frequency (72.265355 MHz on our spectrometer). WURST-80 pulses [10] were generated using the Bruker ShapeTool software. All pulses were applied with CYCLOPS phase cycling. Continuous-wave  $^1\text{H}$  decoupling was applied at  $\nu_1 = 80$  kHz in all cases unless otherwise specified. A pre-acquisition delay (dead-time) of 50-100  $\mu\text{s}$  was required to remove the effects of acoustic probe ringing and to provide a flat baseline after Fourier transformation. Spectra were processed using the NUTS software (Acorn NMR) with exponential apodization and zero-filling. Simulations of (non-spinning) overtone spectra were generated using the

RMNSim software kindly provided by Prof. Philip Grandinetti (Ohio State University) [9]. All such simulations were generated using experimental quadrupolar parameters [11,12] and  $\delta_{\text{iso}}$  and CSA parameters calculated using density functional theory (CASTEP) [13]. All experimental and calculated NMR parameters, as well as the calculation details, are provided in the Supporting Information.

The  $^{14}\text{N}$  static fundamental powder pattern of L-valyl-L-alanine was obtained at 21.1 T on a 900 MHz Bruker Avance II spectrometer ( $\nu_{\text{L}} = 65.03$  MHz) and a home-built double-resonance static probe with a 7.0 mm i.d. coil size (National Ultrahigh-Field NMR Facility for Solids, Ottawa). The WURST-QCPMG pulse sequence [14] was used with eight-step phase cycling and 50  $\mu\text{s}$  WURST-80 pulses swept over a range of 1.0 MHz ( $\nu_1 = 30$  kHz), resulting in an excitation bandwidth of approximately 850 kHz. Continuous-wave  $^1\text{H}$  decoupling of  $\nu_2 = 15$  kHz power was applied for the duration of each scan. The recycle delay was 0.5 s and 50 echoes were acquired in the QCPMG train. 8 sub-spectra were acquired on the low frequency side of the pattern (300 kHz step size), and the high-frequency side was reconstructed by reflection (a strategy justified elsewhere [12]). The spectrum is referenced to solid  $\text{NH}_4\text{Cl}$  at 0 ppm. Individual echoes were co-added prior to Fourier transformation. Absorptive spectra were obtained *via* a magnitude calculation and complete spectra were reconstructed from the individual pieces *via* a skyline projection. Experimental EFG parameters were determined by manually fitting simulations to the experimental spectra using the Dmfit software [15] (see Supporting Information).

All samples were purchased from Sigma Aldrich and used without further alteration, with the exception of L-valyl-L-alanine, which was obtained from Bachem and was recrystallized from  $\text{D}_2\text{O}$  by evaporation at room temperature in order to reduce the effects of  $^1\text{H}$ - $^{14}\text{N}$  dipolar couplings for the ultra-wideline (static) fundamental experiments [11].

### 3. Results and discussion

Figures 1a and 1b show  $^{14}\text{N}$  overtone spectra obtained from a static powder sample of glycine at 11.7 T. Without  $^1\text{H}$  decoupling applied, the signal is broadened beyond detection by  $^1\text{H}$ - $^{14}\text{N}$  dipolar couplings (Figure 1a). However, when this

interaction is decoupled, the  $^{14}\text{N}$  overtone powder pattern is observed. As outlined previously [5,6], the position of this pattern is determined by the second-order quadrupolar interaction (SOQI) and isotropic chemical shift ( $\delta_{\text{iso}}$ ), and its shape is determined by the SOQI, the CSA, the relative orientations of these interactions, and also the experimental conditions (e.g., the angle between the RF coil and the magnetic field,  $54.74^\circ$  for all spectra shown here). A simulation including each of these effects (Figure 1c) shows reasonably good agreement with experiment.

Spectra were also obtained from glycine under 10 kHz MAS. The MAS spectrum obtained without  $^1\text{H}$  decoupling (Figure 1d) shows approximately the same linewidth and signal intensity as the decoupled static spectrum (Figure 1b), demonstrating that MAS averages the  $^1\text{H}$ - $^{14}\text{N}$  dipolar couplings as would be expected. The decoupled MAS spectrum (Figure 1e) shows a significantly increased intensity as well as a slightly narrower linewidth (FWHM = 1.1 kHz) than the decoupled static spectrum (1.4 kHz). Second-order quadrupolar splittings of ca. 500 Hz are visible in the powder pattern. Crucially, the position of the MAS powder pattern is shifted to a higher frequency by ca. 18.5 kHz relative to the static pattern. Spectra recorded at other spinning speeds (Figures 1f and 1g) show that this shift scales linearly with the MAS rate. Such a shift was predicted qualitatively by Marinelli et al., who explained it in terms of the MAS-induced time dependence of the rotating frame [8], but thus far our simulations have been unable to reproduce this effect. Previously reported theoretical analyses also predict strong spinning sideband-like features (i.e., sets of peaks separated by the spinning rate) in MAS overtone spectra [8,9]. We have observed sideband manifolds with very weak intensities under certain excitation conditions (see Supporting Information), but in general these features are absent from our experimental spectra (or at least below the level of the noise).

In each of the spectra discussed above, the transmitter frequency was placed on resonance with the observed signal, and the intensity of the peak was observed to build up with increasing pulse length, in agreement with the very slow nutation rates predicted for overtone magnetization at low to moderate RF powers [8,9]. When the transmitter was moved away from resonance, however, the apparent nutation rate of the overtone signal was observed to increase dramatically, and in a linear fashion with respect to the

offset from the MAS peak position (Figure 2b). This effect was reproduced quantitatively for glycine in simulations of the static spectra (Figure 2a), for example a 50  $\mu\text{s}$  pulse applied at an offset of  $\pm 20$  kHz corresponds to a  $\pi$  pulse in the simulated nutation curve, and resulted in almost no experimental signal, except some extremely low intensity spinning sideband-like features (see Supporting Information). This increased nutation rate could be useful in producing overtone spin-echoes for individual sites, but it will constitute an undesirable complication when the position of the peak is unknown. Moreover, the full spectral range of  $^{14}\text{N}$  overtone signals will be on the order of 100-200 kHz at intermediate magnetic field strengths, and if  $^{14}\text{N}$  overtone MAS experiments are to be applied to samples with multiple sites, this effect will be a serious problem. Standard (rectangular, monochromatic) pulses are also known to exhibit highly restricted excitation bandwidths when applied to overtone spectroscopy [9], a restriction which must be overcome if this experiment is to become routine. Lee & Ramamoorthy have already demonstrated that composite pulses can provide improved excitation bandwidths over standard pulses [16]. Encouraged by our recent success in using frequency-swept pulses to obtain static (fundamental)  $^{14}\text{N}$  powder patterns [11,12], we have tested the use of WURST [10] excitation pulses on  $^{14}\text{N}$  overtone NMR spectra and have found that they function well under both static and MAS conditions. This is clearly illustrated in Figure 2, where WURST excitation pulses with different sweep ranges show broad, uniform excitation profiles in which the offset-dependent nutation rate is absent. While a short (12.5  $\mu\text{s}$ ) standard pulse can also avoid this effect, the WURST pulses also provide an increased signal intensity.

To attempt to put the sensitivity of these experiments into context, we compared the  $^{14}\text{N}$  overtone MAS spectrum of glycine (obtained with a 100  $\mu\text{s}$  standard, on-resonance pulse) with a natural abundance  $^{15}\text{N}$  CP MAS spectrum from the same sample (Figure 3b). Both experiments were acquired in the same timeframe (ca. 20 minutes), and the  $^{14}\text{N}$  overtone spectrum shows a superior signal-to-noise ratio. This comparison is, however, highly sample specific and should not be taken as a general conclusion that the overtone experiment is more sensitive. Various sample-dependent factors such as  $^1\text{H}$  and  $^{14}\text{N}$   $T_1$  relaxation times,  $^1\text{H}$ - $^{14}\text{N}$  dipolar coupling strengths, nitrogen quadrupolar and CSA interactions and the particulars of the pulse sequences used could each significantly

affect the relative sensitivities of these experiments. In this case, the  $^{15}\text{N}$  CP MAS experiment required a longer recycle delay (2.5 s) than the  $^{14}\text{N}$  overtone experiment (0.5 s). It is easy to imagine situations where one of the methods would have a clear advantage; however, we have shown that in the case of glycine their sensitivities are at least comparable. In practice, the use of both approaches will be advantageous; the  $^{15}\text{N}$  experiment provides accurate isotropic chemical shifts which should then allow the second-order quadrupolar shifts to be determined from the  $^{14}\text{N}$  overtone spectrum (provided that the MAS-dependent shift can be accounted for in the simulations).

In Figure 4, the static overtone powder pattern obtained from *L*-proline (Figure 4a) is contrasted with the MAS spectrum (Figure 4d). In proline, the  $^{14}\text{N}$  CSA is significantly larger than in glycine (see Supporting Information), and the simulations in Figures 4b and 4c show the effect that this interaction has on the static overtone lineshape. The MAS overtone spectrum shows a significant narrowing of the pattern width, and its shape matches more closely with the static simulation in which the CSA is neglected (Figure 4c), suggesting that the CSA is averaged by the sample spinning as one would expect. As with glycine, the MAS peak is shifted to a higher frequency (by ca. 17 kHz). Quadrupolar splittings are absent from the powder pattern in this case due to the high value of the quadrupolar asymmetry parameter ( $\eta_Q = 0.98$ ).

To further test the efficacy of WURST pulses in exciting a broad range of overtone signals under MAS, a spectrum was acquired from the dipeptide *L*-valyl-*L*-alanine (VA) under static (Figure 5c) and 10 kHz MAS conditions (Figure 5d). This sample features two nitrogen sites whose overtone signals at 11.7 T are separated by ca. 45 kHz. In the static case, the signal from the amide site (N2) is broadened significantly by the CSA (see the simulation in Figure 5a) and is therefore difficult to observe in the static overtone spectrum due to the experimental dead-time. Under MAS, however, the averaging of the CSA allows the narrow discontinuity of the powder pattern to be clearly resolved. We note that although the level of signal intensity in Figure 5d is approximately equal for both nitrogen sites in VA, in general overtone NMR signal intensities will not be quantitative due to different inherent signal strengths and nutation rates for sites with different quadrupolar interactions. The similar intensity for these sites

is partly a result of the dead-time which causes the loss of broad underlying features for site N2 (see the simulation in Figure 5b).

Also shown, in Figure 5e, is the static fundamental powder pattern of VA, obtained at 21.1 T using the WURST-QCPMG pulse sequence [14]. The contrast between this static powder pattern and the overtone MAS spectrum provides a remarkable illustration of the advantages of MAS overtone NMR spectroscopy in terms of both spectral width and, particularly, resolution. With regards to information content, the static fundamental powder pattern allows an accurate determination of the quadrupolar parameters (see Supporting Information), but is not suitable for measuring  $\delta_{\text{iso}}$  or the CSA parameters, whose effects on the powder pattern are generally too small to resolve. In the MAS overtone spectrum, the peak positions are determined by both the SOQI and  $\delta_{\text{iso}}$ , which scale differently with magnetic field strength and thus will be measurable from spectra obtained at multiple fields. If a high enough signal-to-noise ratio is achieved, the quadrupolar parameters should in principle be measurable from the shapes of the individual overtone powder patterns, particularly where multiple discontinuities are present (*vide infra*).

Finally, Figure 6 shows  $^{14}\text{N}$  MAS overtone spectra obtained using a WURST pulse from crystalline imidazole, which features two nitrogen sites involved in a hydrogen bond. Both sites are well-resolved in the MAS overtone spectrum. The two features arising at ca. 73 and 82 kHz remained at a constant separation as the MAS rate was varied, and are due to two sharp discontinuities in the N2 overtone powder pattern. The red (dotted) spectrum was acquired with a gap in the  $^1\text{H}$  decoupling field of half a rotor period, which interferes with the MAS averaging of the  $^1\text{H}$ - $^{14}\text{N}$  dipolar interaction, partially re-coupling this interaction and thereby significantly reducing the intensity of the N1 peak, which has a much closer proximity to the H-bond proton and thus experiences a much stronger dipolar coupling strength. The N2 peak intensities were unaffected to within the level of the noise. This demonstrates the feasibility of MAS overtone re-coupling experiments, which will aid spectral assignment and could potentially allow the measurement of bond lengths.

#### 4. Summary

We have demonstrated that  $^{14}\text{N}$  overtone spectra can be obtained from powder samples under magic angle spinning conditions. Line-broadening contributions from the CSA and heteronuclear dipolar couplings are significantly reduced by the sample rotation. Spinning sidebands are minimal, though the peaks show a shift to a higher frequency relative to the static spectrum that is linearly dependent on the MAS rate. For standard excitation pulses, the nutation rate of the overtone magnetization shows a strong dependence on the transmitter offset. This problem can be overcome using frequency-swept excitation pulses, which function well under MAS and also provide a superior excitation bandwidth, allowing coverage of the full  $^{14}\text{N}$  spectral range at intermediate to high field strengths. Using a WURST excitation pulse, spectra have been obtained from the dipeptide L-valyl-L-alanine and imidazole, in which the overtone signals from the different nitrogen sites are well-resolved due to differences in isotropic and second-order quadrupolar shifts.

While these preliminary results have demonstrated the considerable potential of  $^{14}\text{N}$  MAS overtone NMR, there remains much scope for further work. The conclusions of previous theoretical studies were that MAS would not be advantageous in overtone NMR spectroscopy [8,9]. These theoretical descriptions, which do not appear to reproduce the MAS spectra reported here, should certainly be revisited in light of these results, and a quantitative explanation for the MAS rate dependent shifts will clearly be required before  $^{14}\text{N}$  interaction parameters can be measured directly from these spectra. Experimentally, the complex nutation behavior of overtone magnetization, the demonstrated importance of the excitation pulse length and offset under MAS, and the successful use of broadband, frequency-swept pulses, suggest that careful tailoring of the excitation pulse could lead to more quantitative spectra as well as improvements in sensitivity. While MAS generally results in overtone powder patterns with sharp discontinuities that can be observed easily with single-pulse excitation, a significant amount of signal remains lost due to the receiver dead-time. A reliable method for producing overtone spin-echoes across a wide bandwidth is therefore highly desirable. Cross-polarization has previously been shown to provide signal enhancements in static overtone spectra [5,6], and could be extended to MAS to provide sensitivity gains and overcome long  $^{14}\text{N}$   $T_{1s}$ . Finally, the averaging of the CSA and dipolar couplings under

MAS opens up the possibility of  $^{14}\text{N}$ -detected recoupling experiments that may aid with spectral assignment or even allow the measurement of bond distances. We are currently pursuing each of these areas and further publications will be forthcoming.

### **Acknowledgements**

The authors are extremely grateful to Prof. Philip Grandinetti for providing software to simulate the static overtone spectra, and for numerous helpful discussions. Access to the 21.1 T NMR instrument was provided by the National Ultrahigh-Field NMR Facility for Solids, Ottawa ([www.nmr900.ca](http://www.nmr900.ca)).

### **Supporting Information**

DFT calculation details,  $^{14}\text{N}$  NMR parameters for all samples studied, overtone spinning sidebands in a glycine spectrum, fit of the static  $^{14}\text{N}$  fundamental powder pattern for VA.

### **References**

- [1] L.A. O'Dell, *Prog. Nucl. Magn. Reson. Spec.* DOI: 10.1016/j.pnmrs.2011.04.001.
- [2] H.J. Jakobsen, H. Bildsøe, Z. Gan, W.W. Brey, *J. Magn. Reson.* DOI: 10.1016/j.jmr.2011.05.015.
- [3] S. Cavadini, *Prog. Nucl. Magn. Reson. Spec.* 56 (2010) 56
- [4] M. Bloom, M.A. LeGros, *Can. J. Phys.* 64 (1986) 1522
- [5] R. Tycko, S.J. Opella, *J. Am. Chem. Soc.* 108 (1986) 3531
- [6] R. Tycko, S.J. Opella, *J. Chem. Phys.* 86 (1987) 1761
- [7] K. Takegoshi, K. Hikichi, *Chem. Phys. Lett.* 194 (1992) 359
- [8] L. Marinelli, S. Wi, L. Frydman, *J. Chem. Phys.* 110 (1999) 3100
- [9] N.M. Trease, P.J. Grandinetti, *J. Chem. Phys.* 128 (2008) 052318
- [10] E. Kupče, R.J. Freeman, *J. Mag. Reson. A* 115 (1995) 273
- [11] L.A. O'Dell, R.W. Schurko, *Phys. Chem. Chem. Phys.* 11 (2009) 7069
- [12] L.A. O'Dell, R.W. Schurko, K.J. Harris, J. Autschbach, C.I. Ratcliffe, *J. Am. Chem. Soc.* 133 (2011) 527

- [13] S.J. Clark, M.D. Segall, C.J. Pickard, P.J. Hasnip, M.J. Probert, K. Refson, M.C. Payne, *Z. Kristallogr.* 220 (2005) 567
- [14] L.A. O'Dell, R.W. Schurko, *Chem. Phys. Lett.* 464 (2008) 97
- [15] D. Massiot, F. Fayon, M. Capron, I. King, S. Le Calvé, B. Alonso, J.O. Durand, B. Bujoli, Z. Gan, G. Hoatson, *Magn. Reson. Chem.* 40 (2002) 70
- [16] D.-K. Lee, A. Ramamoorthy, *Chem. Phys. Lett.* 280 (1997) 501

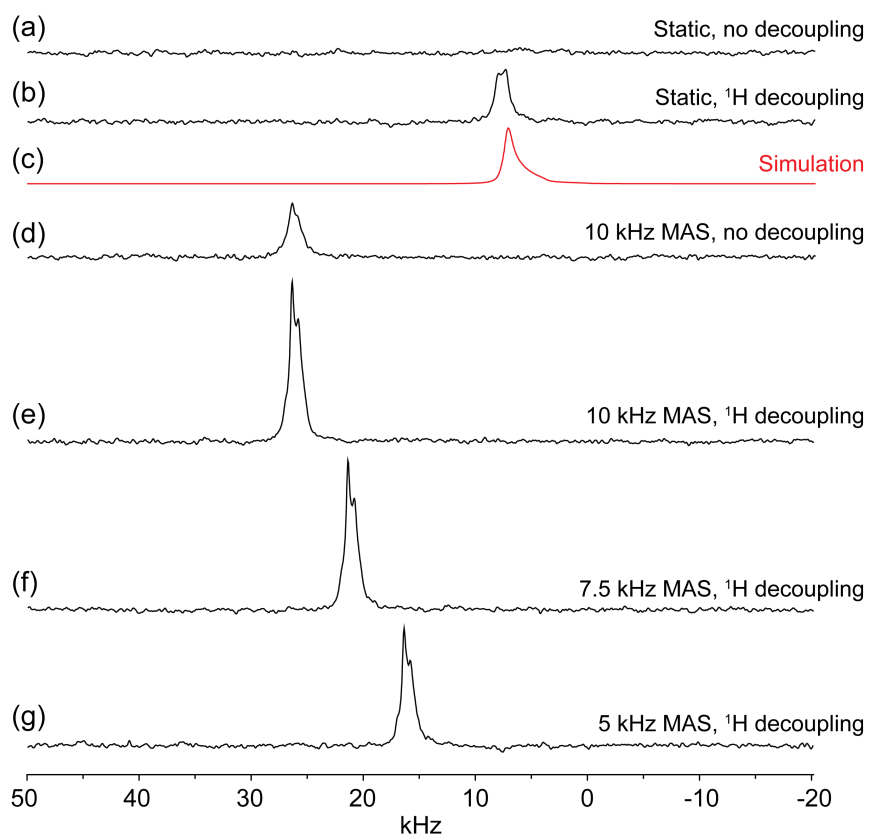


Figure 1 – Overtone  $^{14}\text{N}$  NMR spectra obtained from a powder sample of glycine at 11.7 T under various experimental conditions as indicated on the right. All spectra were obtained with a 100  $\mu\text{s}$  on-resonance pulse, with a recycle delay of 0.5 s and 10,000 scans acquired.

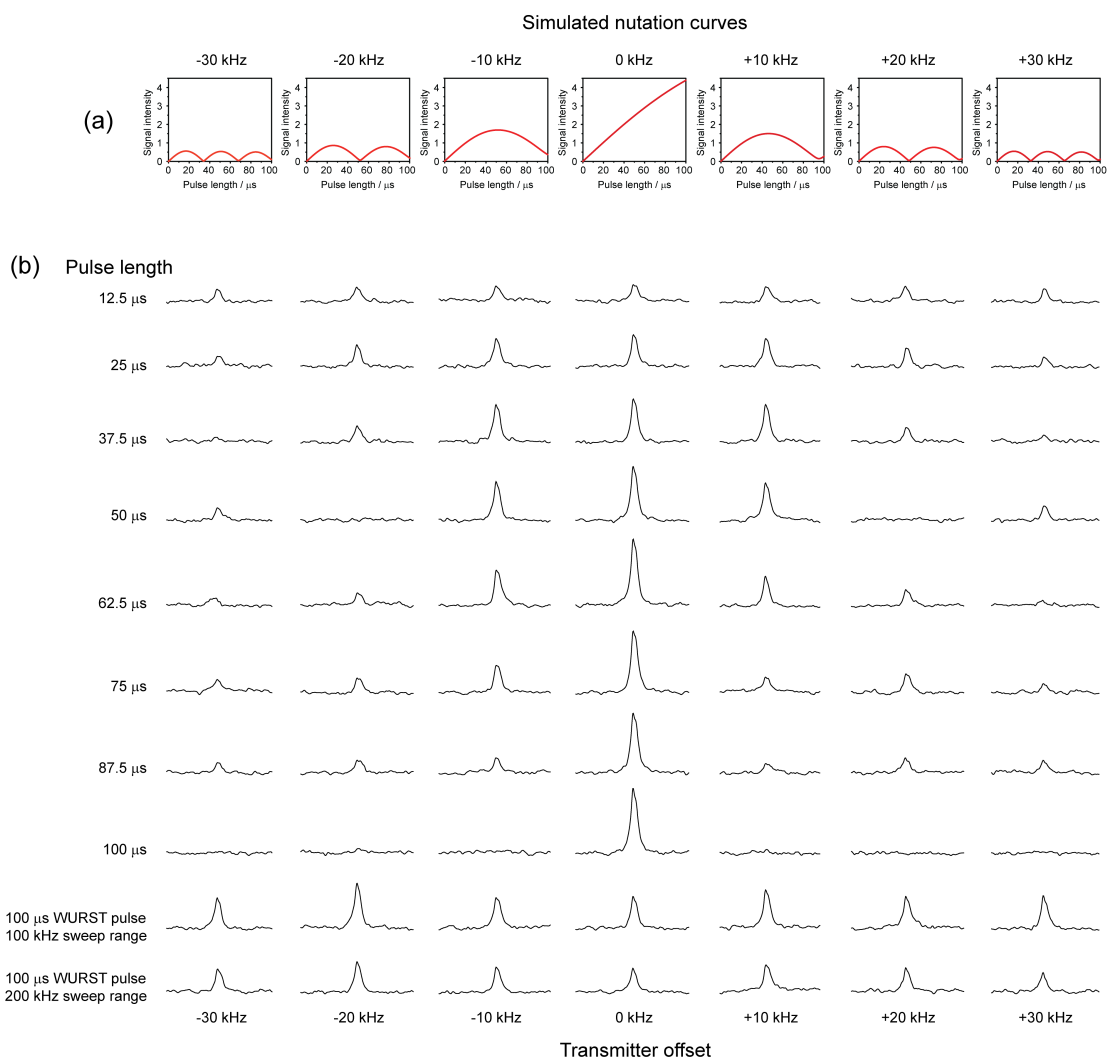


Figure 2 – (a) Simulated static  $^{14}\text{N}$  overtone nutation curves for glycine at 11.7 T with standard (rectangular, monochromatic) RF pulses applied at various offsets relative to the peak maximum ( $\nu_1 = 42$  kHz). The vertical scale represents the relative magnitude of the resulting signal. (b) Experimental  $^{14}\text{N}$  overtone spectra obtained under 10 kHz MAS with pulses applied at the same power and corresponding offsets.

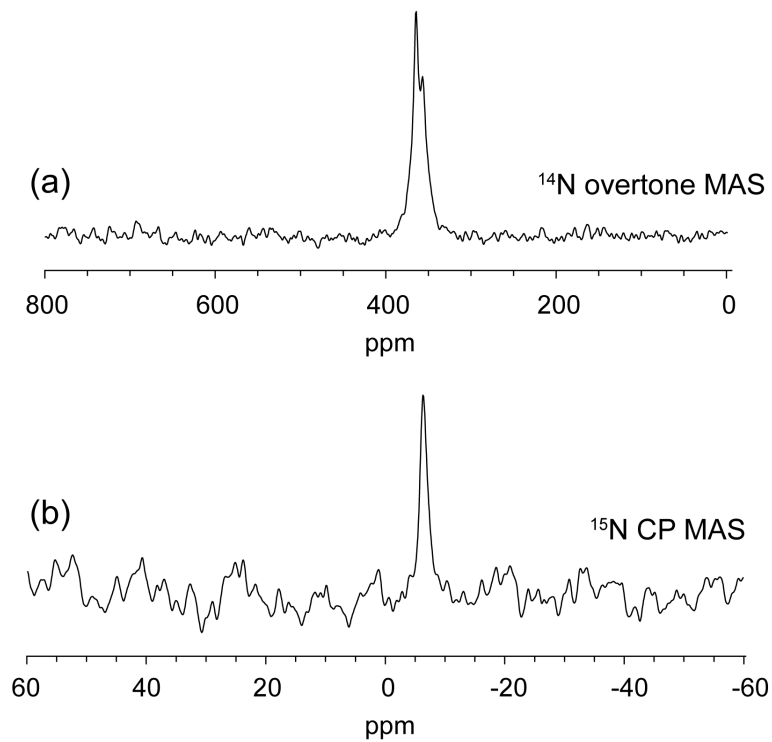


Figure 3 – (a) <sup>14</sup>N overtone MAS spectrum obtained from a natural abundance sample of glycine (2560 scans, 0.5 s recycle delay). (b) <sup>15</sup>N CP MAS spectrum obtained from the same sample in the same experimental time (512 scans, 2.5 s recycle delay). Both spectra were acquired using the same probe at 11.7 T and 10 kHz MAS. The overtone spectrum was acquired with a 100  $\mu$ s on-resonance pulse ( $\nu_1 = 42$  kHz). The <sup>15</sup>N CP parameters (1.5 ms contact time with square contact pulses at  $\nu_1 = 55$  kHz) were set up beforehand on a <sup>15</sup>N-enriched sample of glycine.

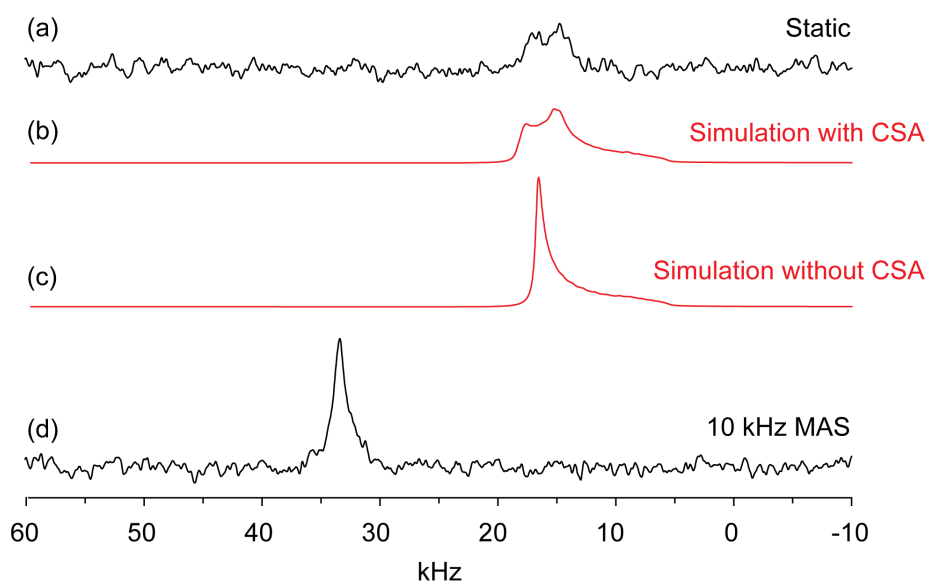


Figure 4 - (a)  $^{14}\text{N}$  overtone NMR spectra obtained from L-proline at 11.7 T under static conditions, (b) a static simulation including experimental EFG parameters and calculated  $\delta_{\text{iso}}$ , CSA and Euler angles (see Supporting Information), (c) the simulation without the effects of the CSA, and (d) an experimental spectrum obtained under 10 kHz MAS. Both experimental spectra were acquired with a 25  $\mu\text{s}$  pulse on resonance, 40,000 scans and a recycle delay of 1 s.

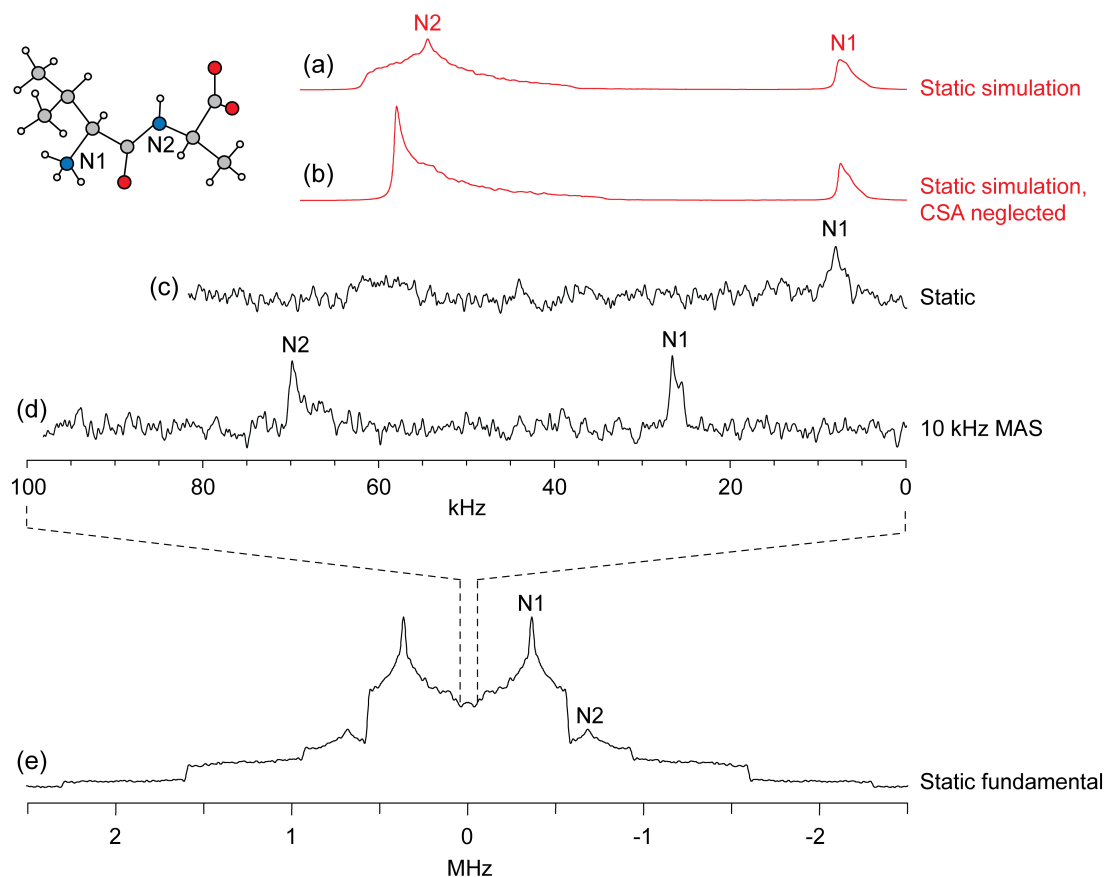


Figure 5 - Simulated static overtone  $^{14}\text{N}$  powder patterns for L-valyl-L-alanine (molecule shown inset) with (a) and without (b) the effects of the CSA, and experimental  $^{14}\text{N}$  overtone spectra obtained at 11.7 T with a  $100\ \mu\text{s}$  WURST pulse swept over a range of 150 kHz under static (c) and 10 kHz MAS (d) conditions. For the experimental spectra, 85,000 scans were acquired with a recycle delay of 0.5 s. A static fundamental powder pattern obtained at 21.1 T with the WURST-QCPMG pulse sequence is shown in (e), and the dashed lines indicate the relative sizes of the frequency scales.

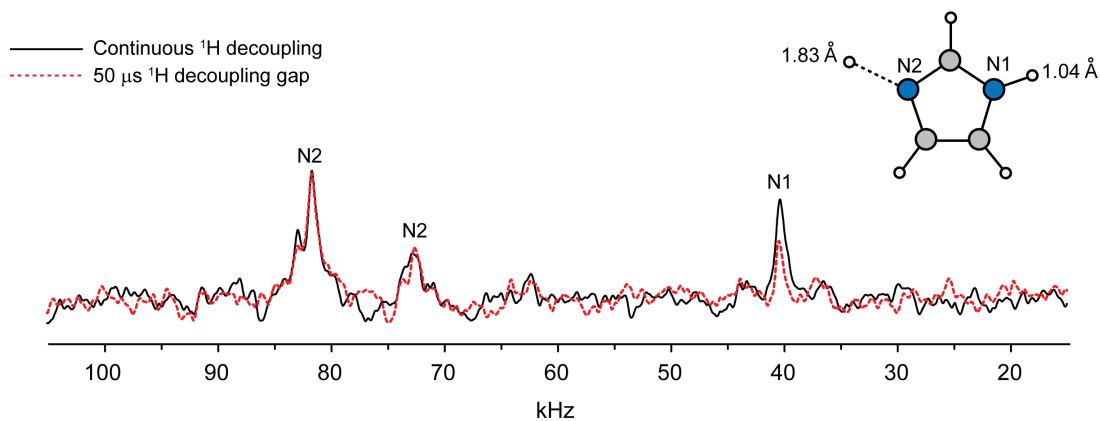


Figure 6 –  $^{14}\text{N}$  overtone spectra obtained from imidazole at 11.7 T and 10 kHz MAS using a  $100\ \mu\text{s}$  WURST excitation pulse swept over a range of 100 kHz. Each spectrum was obtained in 10,000 scans with a recycle delay of 1 s. The black spectrum was obtained with continuous  $^1\text{H}$  decoupling. The red dotted spectrum was obtained under the same conditions but with a  $50\ \mu\text{s}$  gap in the  $^1\text{H}$  decoupling immediately following the excitation pulse. Note that two sharp discontinuities in the N2 powder pattern are visible. The imidazole molecule is shown inset along with the distances to the nearest protons.